Paper presented at the First Topical
Meeting on Fusion Reactor Materials,
Miami Beach, Florida, January 28–31, 1979

Conf-790125--52

ADVANCES IN THE THEORY OF RADIATION EFFECTS IN METALS AND ALLOYS*

L. K. MANSUR and M. H. YOO

Oak Ridge National Laboratory
Oak Ridge, Tennessee 37830

ABSTRACT

Recent advances in the theory of swelling are reviewed. These include (1) the development of a cascade diffusion theory to treat quantitatively the local fluctuations in point defect concentrations, (2) the incorporation of mobile helium into the rate theory, and (3) the spatial variation in swelling during charged particle bombardment.

Large fluctuations in vacancy and interstitial concentration occur at every point during a steady irradiation. The vacancy concentration varies markedly about a fairly uniform background level. The interstitial concentration is nearly always negligible, except for bursts of high levels of short duration, corresponding to the occurrence of a local cascade.

The effect of helium on swelling can be classified into three temperature regimes in terms of the bubble character of the cavities: low bubble character at low temperature (bias-driven swelling), intermediate bubble character at high temperature (gas assisted swelling), and high bubble character (gas-driven swelling). Helium enables swelling at temperatures greater than would be possible without swelling. Reducing the grain size and increasing the dislocation density decrease the swelling caused by helium. This results from the partitioning of helium to these sinks as well as to the cavities.

Three phenomena responsible for spatial variation of swelling during heavy-ion bombardment are assessed. Loss of point defects to the free surface

---

*Research sponsored by the Division of Materials Sciences, U. S. Department of Energy under contract W-7405-eng-26 with the Union Carbide Corporation.

results in only a minor perturbation of swelling under the usual depths and conditions considered. Interstitials injected by the bombarding beam may severely deplete the void volume under certain conditions. The effect is extremely sensitive to defect and materials parameters and is largest for low swelling materials. The previously unexplored depletion of swelling resulting from diffusional spreading of point defects out of the region of maximum energy deposition is evaluated and found to be significant.

1. INTRODUCTION

There have been recent advances in the theory of radiation effects on several fronts. The present paper is devoted to describing recent advances in the theory of void swelling. The topics to be covered also have importance in areas other than void swelling.

Earlier papers of Harkness and Li [1], Wiedersich [2], and Brailsford and Bullough [3] contain the basic form of the present theory of void swelling. Wolfer et al. [4] and Heald [5] have reviewed aspects of the theory at a recent conference. The review and critical assessment of Mansur [6] contains a development of the theory up to about the beginning of 1978. The present paper therefore describes work which has taken place over the past one to two years. In accordance with the theme of this conference, the topics chosen have special relevance to fusion reactor materials. The topics to be covered are the effects on swelling of inhomogeneous point defect production in cascades, of helium gas generation by transmutation reactions or deliberate injection, and of spatial effects during charged particle bombardment.

The mathematical theory needed to describe the ideas discussed in the background sections quantitatively and to obtain the results in the results sections is outlined. The description must be very brief in response to the stringent length limitations for papers in this conference. For reviews of the general development of the theory of void growth see Refs. [4–6]. Section 2 in each of Refs. [7,8,9] contain more complete formulations for inhomogeneous point defect production, gas effect on swelling, and spatial variation of swelling during charged particle bombardment, respectively. Those sections should be incorporated by the reader to supplement the present section.

2. INHOMOGENEOUS POINT DEFECT PRODUCTION

2.1 Background

The theory of swelling has been developed based primarily on chemical reaction rate theory. In this approximation point defect generation is modeled as occurring at all points in a continuum and at a continuous rate during a steady irradiation. After a given time in a volume of material the rate theory generation rate in the continuum equals the physical production rate in the real material. The generation of one point defect in this picture is achieved in effect by the integrated contributions of all points in the continuum each producing an infinitesimal fraction of a defect at a continuous rate. Each point in the continuum has void, dislocation, precipitate, grain boundary, etc., sink character. If the radiation is interrupted, the generation rate at each point in the continuum becomes zero. The populations of vacancies and interstitials decay by mutual recombination and by absorption at every point in the continuum. When radiation is resumed, the populations again build up uniformly.*

In the real material, vacancies and interstitials are produced in discrete atomic units. During neutron or heavy-ion irradiation they are created in cascades by the collisions of bombarding particles with lattice atoms.

---

*The rate theory picture has an equivalent probabilistic interpretation, wherein each point defect is produced as an atomic unit at a specific location. Averaging over large volumes for long times gives the result that the probability of generating a point defect is distributed uniformly in infinitesimal increments to an infinite number of points.

Since such collisions occur randomly, vacancy and interstitial production is inhomogeneous on a local scale. It has been pointed out that this will result in significant local fluctuations in point defect concentrations [6,10]. Spatially localized sinks such as voids and lengths of dislocations are thus subjected to fluctuating vacancy and interstitial fluxes during steady irradiations. Pulsing the radiation source itself superimposes additional fluctuations. In the rate theory approximation, however, there is a qualitative difference between pulsed and steady irradiations. In the steady case the sinks experience no fluctuations in defect fluxes.

There have been a number of applications of the rate theory to the calculation of point defect concentrations as well as to void nucleation and growth during pulsed irradiations [11–16]. Not surprisingly the rate theory leads to the prediction that swelling should be different during pulsed and steady irradiations. For example, it has lead to the conclusion that for certain regimes of pulse interval/duration, little or no swelling would occur where swelling would occur in steady irradiations to the same dose.

We have suggested that it is desirable to understand the effects of the local cascade pulsing of defect fluxes at sinks which occurs during steady irradiations in order to evaluate the effects of superimposed radiation pulsing [6]. This must be done with a theory which has greater resolution than rate theory with respect to point defect production and subsequent diffusion. In sections 2.2 and 2.3 we summarize the development of a theoretical method [7] to treat this problem.

2.2 Theory

The cascades of point defect production are idealized as delta functions occurring at time t_c and position r_c. The diffusion of these cascades is governed by the equation

$$D\nabla^2\tilde{c} - DS\tilde{c} + \delta(\rho - \rho_c)\delta(t - t_c) = \frac{\partial\tilde{c}}{\partial t} \qquad (1)$$

which is satisfied by the Green's function

$$\tilde{c}(\rho|\rho_c,t - t_c) = \frac{1}{8[\pi D(t - t_c)]^{3/2}} \exp[-(\rho - \rho_c)^2/4D(t - t_c)]\exp[-DS(t - t_c)] \quad (2)$$

In these equations ρ denotes the distance from the center of the cascade, t time, $\tilde{c}$ the concentration of vacancies or interstitials, D diffusion coefficient, and S the strength of all sinks modeled as spread through the continuum. In the calculations to be described, cascades are introduced at discrete positions and times throughout the medium as required physically. The concentration of vacancies and interstitials at an arbitrary point resulting from the superposition of contributions from all these cascades, each contributing a value according to equation (2), is computed.

2.3 Results

Consider an arbitrary point in a material under steady irradiation and monitor the concentrations there of vacancies and interstitials. In the rate theory as is well known [6] the point defect concentrations build up after the onset of irradiation to quasi-steady state values determined by the sink strengths and the mutual recombination rate. Following this the only change in these values with time is a gradual decrease to maintain a steady state as the internal sink strengths of voids and dislocations rise in response to the net point defect accumulation (hence the term quasi-steady state). However, the more physically realistic model described in the previous section which accounts for the inhomogeneous nature of point defect production leads to the vacancy and interstitial concentrations shown in Figs. 1 and 2. The conditions represent a typical steady reactor irradiation of stainless steel at 500°C, 10^{-6} dpa.s that contains a dislocation density of 10^{11} cm^{-2}.

The most notable feature in Figs. 1 and 2 is the extreme fluctuation with time in vacancy and interstitial concentrations. For the vacancy concentration there is a roughly steady background concentration punctuated by spikes which raise the instantaneous concentration more than an order of magnitude. These spikes arise from cascades occurring relatively near the point of observation. The background is supplied by a much larger number of more distant cascades. The number of cascades occurring per unit time in a thin spherical shell about the point of observation increases as the square of the radius of the shell, i.e., as the square of the distance from the point of observation. At the same time, the more distant a cascade, the smaller is its contribution to the concentration at the point of observation. A distant cascade will have become dilute spatially by diffusional spreading; and the number of defects surviving absorption at sinks by the time the distant cascade produces a significant contribution at the point of observation is relatively small.

The fluctuations in the interstitial concentration are much more abrupt. Figure 2 shows the interstitial concentration with time where the time axis spans a random interval within which three consecutive cascades have occurred. The istances from the point of observation to the centers of these particular cascades are shown at the top of the figure. Each cascade results in a very fast build-up and decay of interstitial concentration at the point of observation. For these cascades the interstitial concentration rises and decays in fractions of a microsecond, while the individual cascades are separated by several milliseconds. In contrast to the situation for vacancy concentration, therefore, there is at most only one cascade contributing to the interstitial concentration at an arbitrary point of observation at any time.

A brief discussion on the interpretation of these results may be helpful. To monitor the concentration at a point is a mathematical statement. Physical concentration is measured in atomic units. What Figs. 1 and 2 show when the ordinates are reduced by the number of atoms per unit volume, is the probability of finding a vacancy or interstitial at a particular atomic site. This is equivalent in a probabilistic sense to the result of dividing every cascade into an infinite number of infinitesimal fractional defects, a continuum fluid, whose sum equals the number of atomic defects in the cascade. The mathematical treatment here calculates the diffusion of this probability fluid, and we interpret the results in terms of discrete atomic defects. Thus we have used the convenience of a continuum theory in the treatment of diffusion and absorption of defects where this does not obscure the spatially and temporally discrete production of point defects.

These local fluctuations in point defect concentrations during steady irradiations are found to give only small differences compared with rate theory for the growth of voids [7]. This is because the fluctuations make only small relative step changes in the radius of a void. Large fluctuations in the thermal vacancy emission rate do not occur and the fluctuating growth process may be approximated by using average vacancy and interstitial fluxes. For void nucleation or pulsed irradiation conditions the differences with rate theory may be more pronounced. Irradiation creep by climb-enabled glide may also be enhanced by large fluctuations in point defect fluxes to dislocation segments. Creep by climb-enabled glide may be possible in this picture even in the absence of a long-term averaged net climb, since the fluctuating point defect fluxes will produce climb by either net vacancy or net interstitial absorption over short time intervals.

3. EFFECTS OF HELIUM

3.1 Background

Of the nuclear collisions which neutrons undergo in a fusion reactor first wall, a small fraction result in the production of helium by (n.α) reactions. In the structural material of fast fission reactors helium is produced at an order of magnitude lower rate primarily because of lower reaction cross sections at the order of magnitude lower neutron energy. Even at the production rates in fast fission reactors, however, helium is known to produce marked changes in the swelling, embrittlement, and precipitation behavior of structural materials.

Helium has been included in the theory of swelling by accounting for the pressure of transmuted helium in the cavities [17]. Under the high rates of gas production in fusion environments it is expected the swelling will occur at high temperatures by gas driven bubble growth [18]. It has also been recognized that to simulate neutron irradiations using heavy-ion accelerators, the simultaneous injection of helium is necessary. Several facilities for simultaneous helium injection have been developed over the past several years [19]. Theoretical analyses of swelling for various relative rates of helium injection and damage production reveal a marked sensitivity of high temperature swelling to this ratio [20]. The incorporation of gas into both void nucleation and growth in a composite model is described in another paper in this proceedings [21]. Recently, the mobility of helium has been incorporated into calculations of nucleation behavior [22] and has also been included in the theory of void growth [8].

3.2 Theory

The presence and mobility of helium is included in the theory by accounting for the following reactions

$$\mathrm{He}^{I} \xleftarrow{G_g} \mathrm{Matrix}, \tag{3}$$

$$\mathrm{He}^{I} \xrightarrow{K_g} \mathrm{Sinks}, \tag{4}$$

$$\mathrm{He}^{I} + v \underset{K_d}{\overset{K_a}{\rightleftarrows}} \mathrm{He}^{S} , \tag{5}$$

$$\mathrm{He}^{S} + i \xrightarrow{R'} \mathrm{He}^{i} . \tag{6}$$

The superscripts I and S denote interstitial and substitutional positions of He and the terms v and i denote vacancies and interstitials. The reaction constants G_g, K_g, K_a, K_d, and R' denote respectively generation of He^I, loss of He^I to internal sinks, trapping of He^I by v, release of He^I from v and the annihilation by i of He^S-occupied v to give He^I. The rate equations governing point defect concentration and void growth may be generalized to incorporate these reactions in a straightforward manner [8].

3.3 Results

Void growth with helium present is illustrated as a function of temperature in Fig. 3. Conditions are typical for nickel in a fusion reactor first wall at 10 dpa, dose rate 3.9×10^{-7} dpa/s and gas transmutation rate of 1.3×10^{-11} apa/s. Cases (a), (b), and (c) represent increasing degrees of refinement in accounting for helium behavior. The dashed curve is the case with no helium and it is seen that the high temperature cutoff of swelling is at $\sim 0.5\ T_m$. In curve (a), all helium generated is modeled as contained in cavities. The swelling is not cut off but reaches a minimum between 0.5 and 0.6 T_m and then increases at higher temperature. In curve (b) the gas is allowed to partition itself among voids, dislocations, and grain boundaries according to the strengths of these sinks for point defects [6]. In curve (c) the calculation includes partitioning and the additional process of helium-vacancy trapping and associated reactions as described in the previous section. Partitioning and trapping are found to decrease the swelling at high temperatures compared to that obtained by assuming all helium to be generated in the cavities.

To help understand the effects of gas we have developed plots displaying the bubble character of the cavities. The upper part of Fig. 4 shows the swelling case (c) of Fig. 3 for reference as well as two additional cases corresponding to swelling during self-ion bombardment at a rate 10^4 times that of case (c) of Fig. 3. In Fig. 4 curve (a) has simultaneous helium injection at a rate 10^4 that of curve (c) of Fig. 3, and curve (b) has preinjected helium. The lower part of Fig. 4 shows the bubble character of the cavities. We define bubble character as the ratio of the number of gas atoms in the cavities to the number that would be contained in an equilibrium bubble of the same radius. At 0.4–0.5 T_m the bubble character is low, indicating that the cavities are growing as a result of the net dislocation bias-driven growth.

Below these temperatures the bubble character is higher because the cavities are smaller, but the cavities still grow due to the bias since thermal vacancy flux is not a consideration. In the temperature range 0.5–0.6 T_m the bubble character increases but does not equal unity. By comparison with the gas-free case of Fig. 3 it necessarily follows that cavities exist in this region as a result of gas-assisted growth. In this region bubble growth takes place by the continuous incorporation of helium and vacancies — gas-driven bubble growth — until the cavities reach a critical size beyond which bias driven growth is possible.* The critical size corresponds to that radius for which the sum in curly brackets in eq. (9) just equals zero with the thermal vacancy concentration dependence on gas pressure given by eq. (10). In the temperature region above about 0.6 T_m the bubble character equals unity. In this regime, only gas-driven bubble growth is possible. The thermal vacancy flux even from a flat surface (a cavity of infinite radius) exceeds the net radiation-produced vacancy flux in the absence of gas, and cavity growth is only possible by the continuous incorporation of gas and vacancies in a ratio appropriate to an equilibrium bubble. Figure 5 illustrates the effects of varying the dislocation density and the grain diameter. The upper part of the figure shows the swelling as a function of

---

*Recall that the thermal vacancy concentration at a void of radius r_V, $C_V^e(r_V)$ depends exponentially on the inverse of the void radius, see eq. (10).

temperature for three dislocation densities. L denotes the dislocation density used for the calculations of Figs. 3 and 4. It is a temperature dependent function [8] based on the experimental observations of Packan, Farrell, and Stiegler in nickel [23]. The curves denoted 2L and L/2 show the swelling with multiples of that function. A higher dislocation density results in higher swelling in the bias-driven swelling regime under these conditions, but this dependence is reversed in the gas-driven swelling regime. The explanation is that the additional dislocations act as gas sinks in the gas-driven regime and, therefore, eliminate part of the driving force for gas-driven swelling. These additional dislocations increase the net vacancy influx to cavities by their net absorption of interstitials in the lower temperature bias-driven regime, however, where gas is unimportant.*

The relative effectiveness of grain boundaries as point defect sinks and gas sinks is even more dramatic,as shown in the lower part of Fig. 5. The grain diameter is varied from 100 to 5 μm. In the bias-driven regime the effect is small, indicating that the proportion of point defects lost to grain boundaries to that lost to all other processes is small. However, at small grain diameters the effect on gas-driven swelling is large, indicating that small grain-size

---

*This behavior has been predicted analytically [6]. However, it is important to understand that the swelling response to changes in dislocation density in the bias-driven regime is determined by the relative importance of losses of point defects to voids, dislocations, and recombination. For example, where dislocations are the dominant sink and mutual recombination is unimportant, increasing the dislocation density in the bias-driven swelling regime will decrease the swelling [6].

materials should have much lower gas-driven swelling. A large proportion of the total helium is lost to grain boundary sinks and the gas-driven swelling is reduced substantially. In the bias-driven regime, however, the proportion of point defects lost to grain boundaries is small in comparison to the total loss, which includes a large recombination loss in addition to losses to voids and dislocations.

4. SPATIAL VARIATION IN VOID VOLUME DURING CHARGED PARTICLE BOMBARDMENT

4.1 Background

The possibility has long been recognized that the free surface of the specimen, being typically of order one micron from the region of interest in charged particle experiments, could reduce the swelling by acting as a competing sink for point defects. More recently two additional effects which are associated with heavy-ion bombardment have been identified.

The first arises from the injection of the bombarding ions as self-interstitials directly into the region of interest. That this effect could be important was established analytically in Ref. [24]. Under the conditions considered in [24], a depletion of void volume ranging from ones to tens of percent was expected, depending on the conditions. These results were also confirmed by spatially dependent numerical computations [25]. However, the sensitivity of void volume depletion by this mechanism to materials and defect parameters is great, and much larger depletions are possible as are much smaller depletions within the range of physically acceptable parameters [6,24]. This sensitivity is at the heart of the apparently divergent results predicted elsewhere [26]. Therefore, in section 4.3 of the present paper a full physical explanation of the effect is given together with quantitative maps of the void volume depletion as functions of the most sensitive parameters.

The other effect producing a depletion of swelling during heavy-ion bombardment we term diffusional spreading. It arises from the sharp peak in point defect generation with depth during heavy-ion bombardment. Some of the defects diffuse out of this region before being absorbed at sinks. This results in the spreading of the swelling profile with respect to the defect generation profile and a concomitant reduction in the magnitude of the swelling in the peak region with respect to that expected on the basis of the point defect generation profile allowing for no diffusion. The effect is also of practical significance since swelling obtained experimentally at the depth of the peak in point defect generation has generally been related directly to the displacement rate at the peak without accounting for the depletion of swelling by diffusional spreading. Thus, if all other differences were to be properly accounted for, this effect would lead to a lower swelling rate/displacement rate ratio for heavy ion bombardment than for neutron irradiation with its spatially uniform displacement rate.

4.2 Theory

In the basic rate theory, the conservation equations for vacancies and interstitials may be written

$$D_v\nabla^2C_v + G_v - RC_vC_i - K_vC_v = \frac{\partial C_v}{\partial t} \quad , \tag{7}$$

$$D_i\nabla^2C_i + G_i - RC_vC_i - K_iC_i = \frac{\partial C_i}{\partial t} \quad . \tag{8}$$

The first terms describe diffusional leakage, the Gs are the generation rates of defects per unit volume, the terms containing R, the recombination coefficient, describe losses by mutual recombination, and the last terms on the left describe losses to internal sinks such as voids and dislocations. D denotes diffusion coefficient, C point defect concentration per unit volume, and K = SD denotes the loss rate per defect to sinks of strength S. Subscripts v and i denote vacancies and interstitials, respectively. These equations are solved simultaneously with the following equation in a fully spatially dependent computation to obtain the growth rate of a void of radius r_V [27].

$$\frac{dr_V}{dt} = \frac{\Omega}{r_V} \left\{ Z_v^V(r_V) D_v [C_v - C_v^e)] - Z_i^V(r_V) D_i C_i \right\} \quad . \tag{9}$$

Here Ω is atomic volume, and Z^V is void capture efficiency. $C_v^e(r_V)$ is the thermal equilibrium vacancy concentration at a void of radius r_V,

$$C_v^e(r_V) = C_v^e \exp\left[\left(\frac{2\gamma}{r_V} - p_g\right) \Omega/kT\right] \quad , \tag{10}$$

where C_v^e is the bulk thermal vacancy concentration, γ is surface tension, p_g is the pressure of gas in the cavity and kT is the Boltzmann factor.

The first two terms in eqs. (7) and (8) lead to the spatial dependence discussed in this paper. The first term accounts for diffusional losses to the free surface of a bombarded specimen, which depletes the swelling near the surface. It also accounts for the diffusional spreading of point defects that occurs during heavy-ion bombardment because of the spatially peaked generation of point defects near the end of the ion range. The second term in eq. (8) may be written $G_i = G(1 + \varepsilon_i') = G + G_i'$ where G is the radiation-produced rate of interstitial generation, and ε_i' is the additional fractional generation rate of self-interstitials from the injection of bombarding ions. Both G and G' have a pronounced spatial dependence (see Fig. 8). The spatial variation in G gives rise to diffusional spreading; and G_i' and its spatial variation account for a significant and spatially dependent depletion of void volume.

4.3 Results

In thin foil irradiations in the high voltage electron micorscope the damage rate is nearly uniform, and the main spatial variation in swelling arises from the presence of the free surfaces. During heavy-ion bombardment of thick specimens the range of the bombarding particles is short, and the damage rate is nonuniform leading to the two additional sources of spatial variation described in section 4.1. Figure 6 shows the effect of diffusional spreading. The upper part is for 650°C while the lower part is for 550°C. In both cases the peak effective point defect generation rate is 1.4×10^{-3} dpa/s. These calculations represent the growth rate of a void of 10 nm radius when placed at various depths in 4 MeV Ni ion bombarded nickel. The horizontal line represents the result for an irradiation in an infinite medium at a uniform generation rate of 1.4×10^{-3} dpa/s. Each point on the dashed curve represents the growth rate of a void in an infinite medium with a uniform dose rate at each point corresponding to the profile for 4 MeV Ni on nickel, i.e., using an infinite medium rate theory. The solid curve represents the swelling rate obtained using the fully spatially dependent model that has been developed recently and described in Ref. [27]. The departure of the solid curve from the dashed curve is caused by diffusional spreading. The departure near the peak is quite pronounced. The position of the peak, however, is not changed significantly. This effect also produces a low level of swelling well beyond the peak in energy deposition. The swelling rate at the peak damage depth for a given dose rate is lower than expected on the basis of a model which only accounts for the spatial variation in point defect generation rate. The significance of this is that the swelling rate/dose rate ratio near the peak in an ion bombardment experiment when all other effects are accounted for will be lower than in a neutron irradiation experiment because of diffusional spreading in the former case. This effect should be taken into account in attempts to correlate neutron and heavy-ion induced swelling.

The departure of the solid curve from the dashed curve near the surface measures the depletion caused by loss of point defects to the surface. To demonstrate this the results of a second calculation are shown in Fig. 7. To clearly separate the effect of diffusional spreading from the surface effect this calculation employs a uniform generation rate of 1.4×10^{-3} dpa/s. Thus any curvature in the swelling rate plot can only be due to the free surface. The upper part shows the result for 650°C at the very low dislocation density of 1.4×10^{9} cm^{-2}. Even for this extreme case the depletion at the depth of peak dose rate, ~0.7 μm, is about 8%. For the more reasonable but still relatively low dislocation density of 1.4×10^{10} cm^{-2}, the depletion caused by the surface is negligible beyond a depth of about 0.4 μm.

Superimposed on these effects will be the depletion of void volume caused by injected interstitials. Figure 8 shows the depletion caused by injected interstitials at two temperatures. The upper part shows the defect generation rate and ion injection rate profiles. The middle and bottom parts show the void volume with (solid) and without (dashed) injected interstitials at 600 and 700°C, respectively. Again the temperature dependent dislocation density based on the observations in Ref. [23] is used. For these conditions, injected interstitials cause a large depletion in void volume.

It is important to understand the physical basis of these results. In general it can be said that the injected interstitial effect is small when most point defects generated by irradiation are absorbed at sinks and that is is important when most are lost to recombination. This occurs because regardless of the fates of vacancies and interstitials generated by irradiation, a number of interstitials equal to the number of injected interstitials must be absorbed at sinks. There are no corresponding vacancies with which these can recombine. Thus where recombination dominates point defect loss, the point defects absorbed at sinks contain a large proportion of injected interstitials. A fraction of these are partitioned to voids according to the sink strength of voids relative to the total sink strength and thus reduce the void volume.

Three important material properties affecting the fraction of point defects recombining in the matrix are the bias, the vacancy migration energy and the sink strength. Figure 9 displays effect of injected interstitials on the void growth rate in that portion of the vacancy migration energy-bias field which covers the current range in these parameter values used in various calculations in the literature. What is plotted is the ratio of the void growth rate with, to that without injected insterstitials, each calculated with the vacancy migration energy and bias corresponding to the projected point on the two dimensional vacancy migration energy-bias plane below. Any magnitude of effect is possible, ranging from negligible to complete void growth suppression. For a given set of parameters the effect is more important for lower sink strengths. Figure 10 shows the ratio of void growth rate with to that without injected interstitials as a function of sink strength for several values of vacancy migration energy. At low sink strengths the depletion is large. In Ref. [9], possibly the first experimental observations of the injected interstitial effect are described. The depletion was found to be substantial and to be strongly dependent on sink strength.

5. SUMMARY AND DISCUSSION

A theoretical method has been devised which resolves individual cascades to determine the local fluctuations in point defect concentrations caused by microscopically inhomogeneous and discontinuous point defect production. The large fluctuations in vacancy and interstitial concentration that occur with time in any arbitrary region have been evaluated quantitatively. In a particular application of the method to the growth of voids of typical size (10 nm radius), only a small difference with the results obtained by using rate theory expressions for vacancy and interstitial concentrations is obtained [7].

Further application of the method to void nucleation and irradiation pulsing are expected to enable further comparisons with rate theory. Implications for irradiation creep may also be important. Such large local fluctuations in point defect concentration may enable dislocation unpinning from obstacles where this would not be reproduced with equivalent steady rate theory concentrations of point defects.

The generation of helium by transmutation and by deliberate injection is accounted for in the theory of void growth. Its presence enables swelling at temperatures much higher than would otherwise be possible. The partitioning of helium to sinks other than voids and its retention in the matrix by vacancy trapping reduce swelling at high temperatures. In particular, significant reductions in the gas driven high temperature swelling are possible when high densities of dislocations and grain boundaries are introduced. Three temperature regimes of swelling can be characterized as bias-driven, gas-assisted and gas-driven. The regimes are understood in terms of the bubble character of cavities as a function of temperature, this being low at low temperatures, intermediate and increasing at higher temperatures, and unity (or 100%) at high temperatures. To make simultaneous heavy-ion bombardment/helium injection experiments yield results more closely approximating fusion reactor irradiations, it is necessary to control the relative rates of gas and heavy-ion impingement carefully. Heavy-ion bombardment experiments using preinjected helium are not expected to reproduce the high temperature gas-driven bubble swelling regime.

The effects of the gas on the dislocation behavior by affecting climb rates, for example, and on grain boundaries by promoting intergranular fracture are recommended as areas for further research. Calculations of the present type, which incorporate the mobility of helium, can serve to provide the essential gas source terms in such further studies.

The spatially dependent rate theory is necessary to predict accurately the swelling behavior that occurs during charge particle bombardment experiments and to relate this information to bulk neutron irradiation experiments that can be analyzed with the simpler infinite medium rate theory. The results may be summarized as follows.

The reduction of swelling due to the free surface is small near the peak in energy deposition (∿0.7 μm) during 4 MeV heavy-ion bombardment. The effect becomes more pronounced at higher temperatures and lower sink strengths. A potentially larger depletion of swelling at the position of the peak in energy deposition can arise from the phenomenon of diffusional spreading of the point defects generated at higher rates near the spatial peak in energy deposition than in the surrounding regions. A large depletion of void volume near the peak in point defect production can also be caused by the injection of the bombarding ions as self-interstitials. The effect is large where point defect recombination dominates point defect loss and small where absorption at sinks dominates. This makes the effect more important in systems with low bias, low sink strength, and high vacancy migration energy. Therefore, the effect is expected to be more important in low swelling materials. Differing predictions of various researchers, covering the range from very small to very large depletions in swelling can be understood as a consequence of different choices of values for these particularly sensitive parameters. By reducing the void volume near the peak in energy deposition the injected interstitials effectively shift the spatial peak in swelling toward the free surface. Recent experimental observations are consistent with a strong reduction in void volume arising from this effect in neutron preirradiated 316 stainless steel [9].

Acknowledgment

The helpful comments on the manuscript of Drs. J. O. Stiegler of ORNL and M. R. Hayns of Harwell are appreciated.

6. REFERENCES

[1] S. D. Harkness and Che-Yu Li, *Metall. Trans.* 2 (1971) 1457.

[2] H. Wiedersich, *Radiat. Eff.* 12 (1972) 111.

[3] A. D. Brailsford and R. Bullough, *J. Nucl. Mater.* 44 (1972) 121.

[4] W. G. Wolfer, L. K. Mansur, and J. A. Sprague, *Proc. Int. Conf. on Radiation Effects in Breeder Reactor Structural Materials,* June 19–23, 1977, p. 841, M. L. Bleiberg and J. W. Bennett, eds. (American Institute of Mining, Metallurgical and Petroleum Engineers, 1977).

[5] P. Heald, see Ref. 4, p. 781.

[6] L. K. Mansur, *Nucl. Technol.* 40 (1978) 5.

[7] L. K. Mansur, W. A. Coghlan, and A. D. Brailsford, this conference.

[8] M. H. Yoo and L. K. Mansur, this conference.

[9] E. H. Lee, L. K. Mansur, and M. H. Yoo, this conference.

[10] Che-Yu Li, D. G. Franklin, and S. D. Harkness, *Irradiation Effects on Structural Alloys for Nuclear Reactor Applications,* ASTM-STP-484, p. 347, (American Society for Testing and Materials, 1970).

[11] J. O. Shiffgens, N. J. Graves, and D. G. Doran, *Proc. Int. Conf. on Radiation Effects and Tritium Technology for Fusion Reactors,* October 1–3, 1975, p. I-532, J. S. Watson and F. W. Wiffen, eds., CONF-750989.

[12] Y. H. Choi, A. L. Bement, and K. C. Russell, see Ref. 8, p. II-1.

[13] N. Ghoniem and G. L. Kulcinski, *J. Nucl. Mater.* 69 and 70 (1978) 816.

[14] G. R. Odette and R. Myers, *CTR Quart. Prog. Rept.,* April–June 1975, HEDL TME/7590, p. 2.

[15] G. J. Dienes, *Rad. Eff.* 36 (1978) 101.

[16] N. Q. Lam, G. Leaf, and R. A. Johnson, *J. Nucl. Mater.* 74 (1978) 277.

[17] A. D. Brailsford and R. Bullough, *Physical Metallurgy of Reactor Fuel Elements,* September 2–7, 1973, p. 148, J. E. Harris and E. C. Sykes, eds., The Metals Society, London.

[18] R. Bullough and M. R. Hayns, see Ref. 11. p. I-230.

[19] Workshop on Use of Dual-Ion Beams in Basic Radiation Effects Research, April 12—13, 1978, Oak Ridge, Tennessee. No published proceedings.

[20] M. R. Hayns, M. H. Wood, and R. Bullough, *J. Nucl. Mater.* 75 (1978) 241.

[21] G. R. Odette, this conference.

[22] B. O. Hall, this conference.

[23] N. H. Packan, K. Farrell, and J. O. Stiegler, *J. Nucl. Mater.* 78 (1978) 143.

[24] A. D. Brailsford and L. K. Mansur, *J. Nucl. Mater.* 71 (1977) 110.

[25] M. H. Yoo, *J. Nucl. Mater.* 79 (1979) 135.

[26] M. R. Hayns, *J. Nucl. Mater.* 78 (1978) 229.

[27] M. H. Yoo, *J. Nucl. Mater.* 68 (1977) 193.

Figure Captions

Fig. 1. Vacancy concentration as a function of time during a steady irradiation.

Fig. 2. Interstitial concentration as a function of time during a steady irradiation. Distances shown correspond to the distances of the particular cascade from the point of observation.

Fig. 3. The effect of helium on swelling. The dashed curve corresponds to the gas-free case. The cases (a), (b), and (c) correspond, respectively, to all gas in cavities, gas partitioned among the sinks, and gas partitioned among the sinks with simultaneous vacancy-helium trapping.

Fig. 4. Swelling (above) with the bubble character of the cavities (below) as functions of temperature. The solid curves correspond to a fusion reactor first wall condition, and the dashed curves (a) and (b) correspond to charged particle bombardments with simultaneous helium injection and helium preinjection, respectively.

Fig. 5. The effect on swelling of variations in the dislocation density (above) and grain diameter (below).

Fig. 6. Calculation of the void growth rate illustrating diffusional spreading. Dashed horizontal line is the infinite medium void growth rate. Dotted curved line is the void growth rate profile obtained from the point defect generation profile when diffusion is ignored. The solid curve is calculated using the spatially dependent theory. The upper part shows results for 650°C and the lower part shows results for 550°C.

Fig. 7. The effect of the free surface on the swelling rate. The upper part shows results for a dislocation density of 1.4×10^9 cm^{-2} and the lower part for a dislocation density of 1.4×10^{10} cm^{-2}. The temperature is 650°C.

Fig. 8. The reduction of void volume caused by injected interstitials. The dashed curves show the void volume without injected interstitials. The solid curves show the void volume when injected interstitials are included. The upper part shows point defect generation and ion deposition profiles, the middle part shows the void volume at 600°C, and the bottom part shows the void volume at 700°C.

Fig. 9. Three-dimensional plot showing the ratio of void growth rate with to that without injected interstitials as a function of bias and vacancy migration energy.

Fig. 10. The void growth rate with to that without injected interstitials as a function of sink strength for several values of the vacancy migration energy.

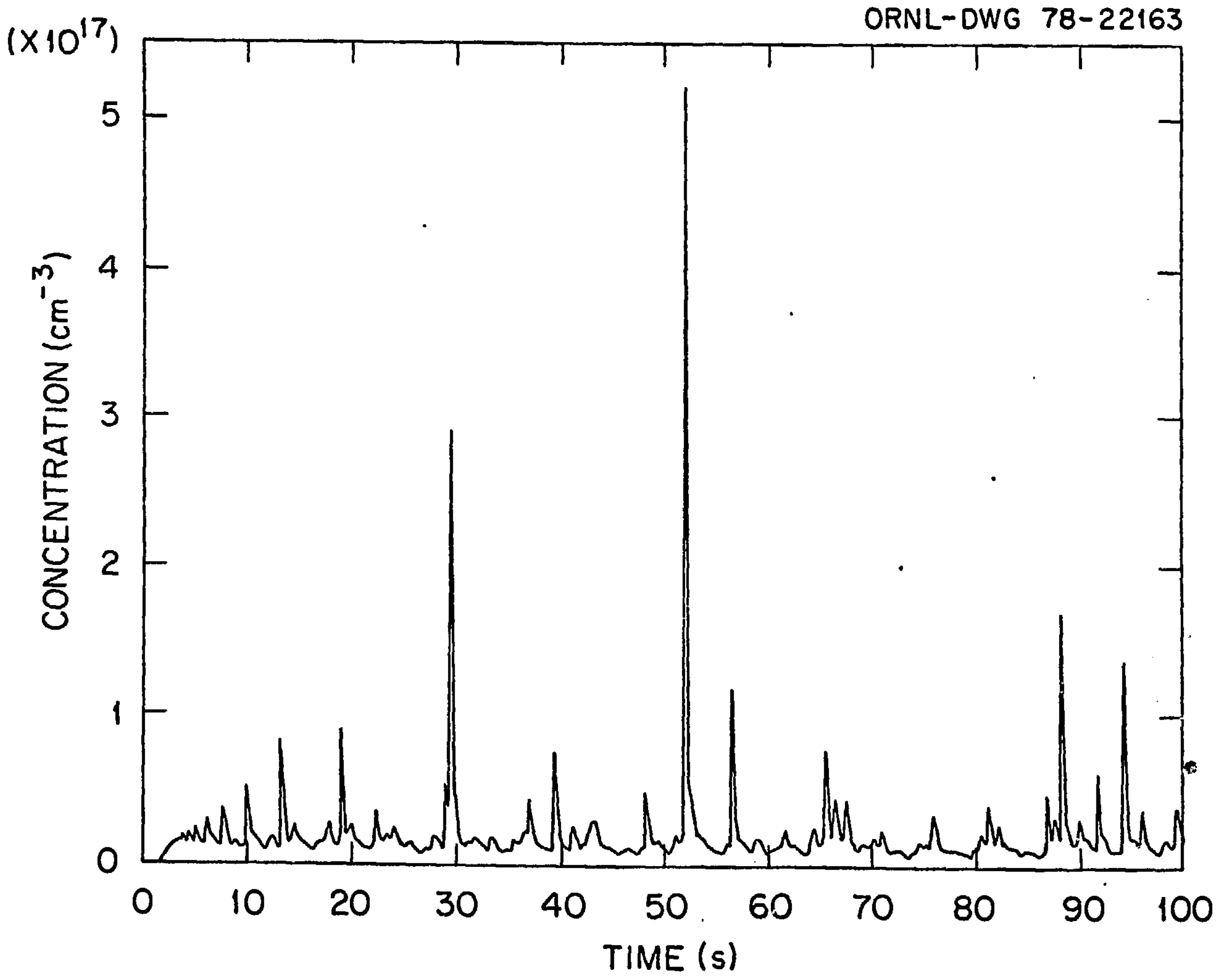
ORNL-DWG 78-22163
(X10^17)
CONCENTRATION (cm^-3)
0
1
2
3
4
5
TIME (s)
0
10
20
30
40
50
60
70
80
90
100

ORNL-DWG 79-7651

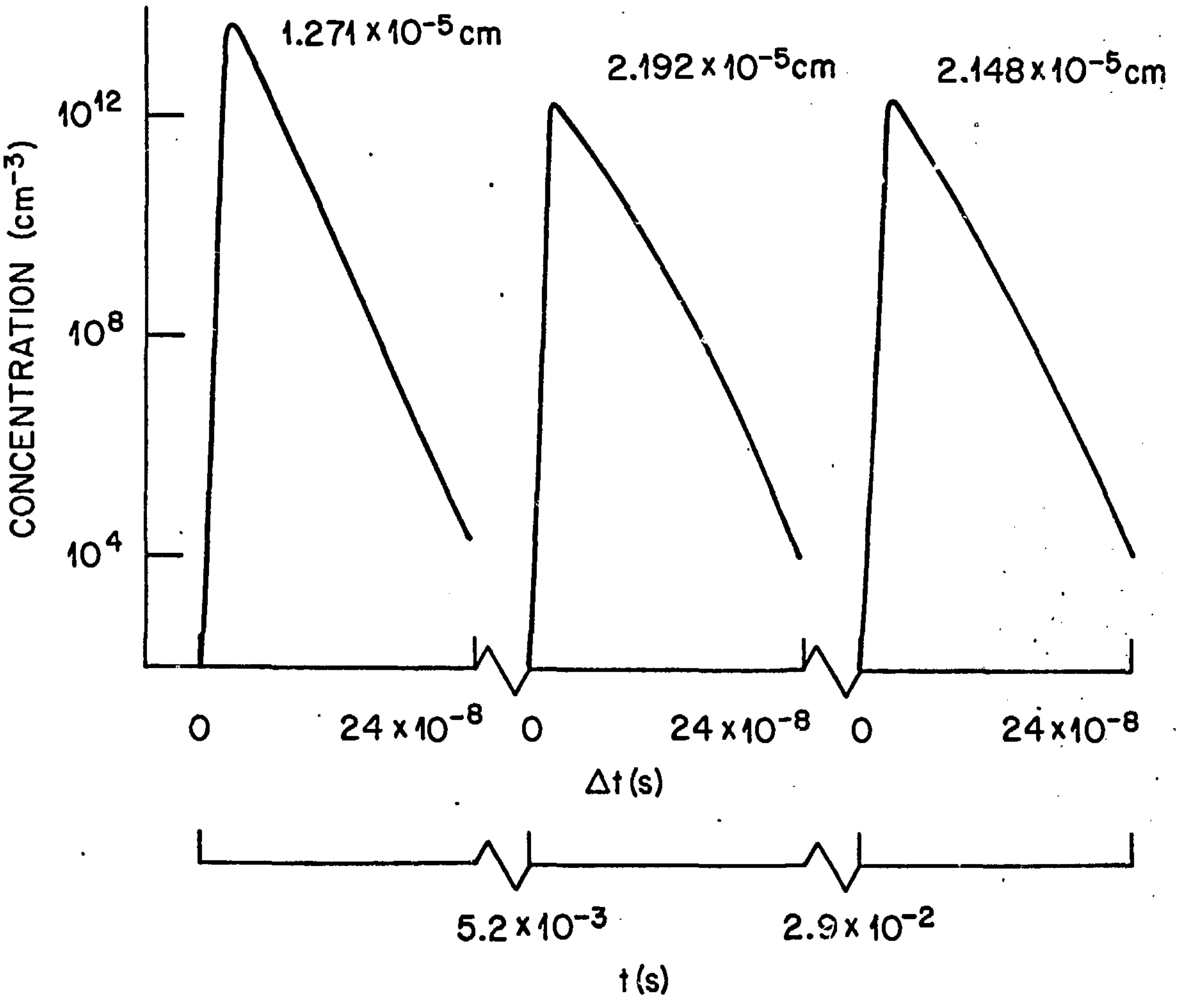

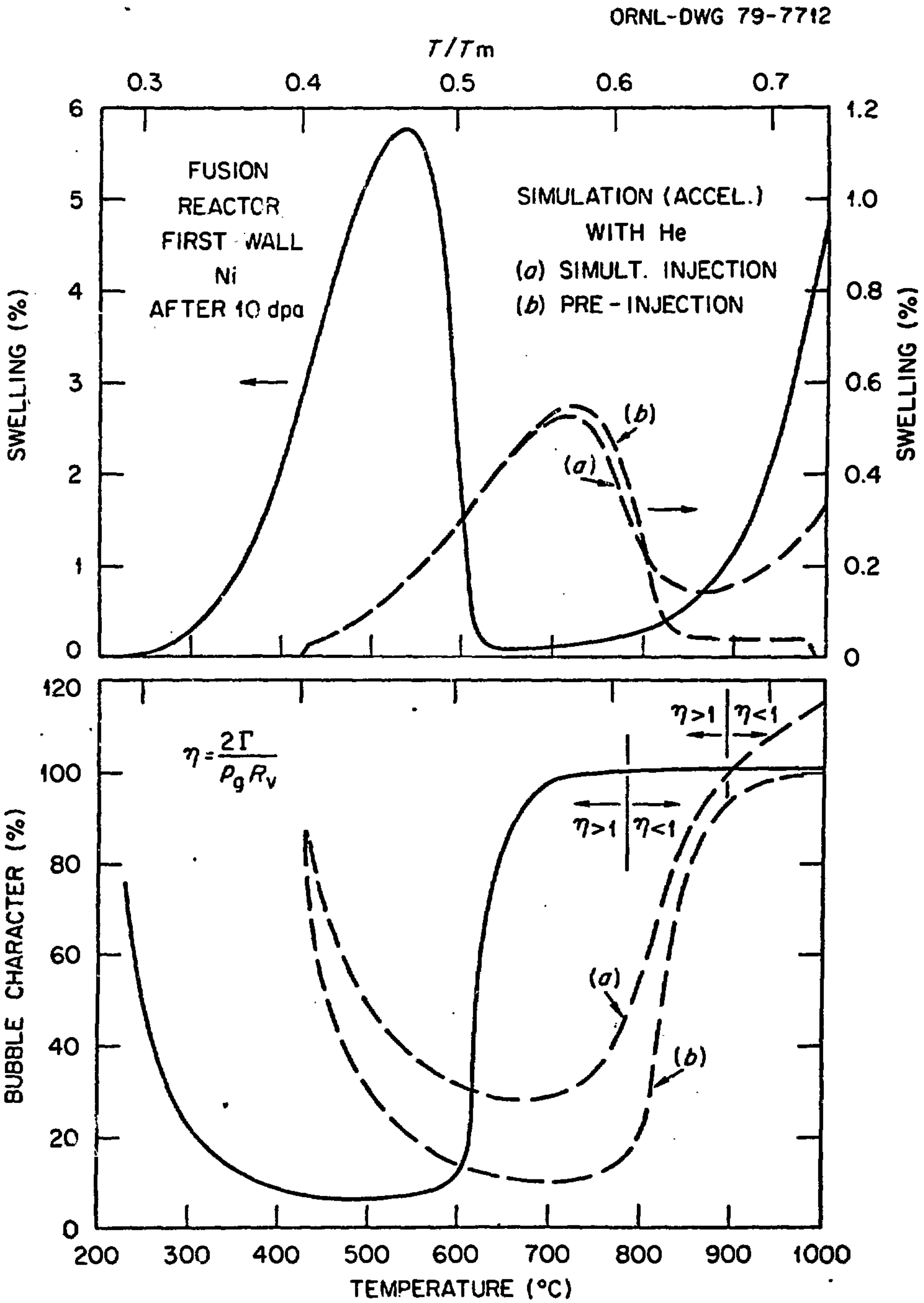ORNL-DWG 79-7712
T/Tm
0.3
0.4
0.5
0.6
0.7
SWELLING (%)
0
1
2
3
4
5
6
1.2
1.0
0.8
0.6
0.4
0.2
0
FUSION REACTOR FIRST WALL Ni AFTER 10 dpa
SIMULATION (ACCEL.) WITH He
(a) SIMULT. INJECTION
(b) PRE-INJECTION
(a)
(b)
BUBBLE CHARACTER (%)
0
20
40
60
80
100
120
η = 2Γ / P_g R_v
η>1
η<1
η>1
η<1
(a)
(b)
200
300
400
500
600
700
800
900
1000
TEMPERATURE (°C)

ORNL-DWG 79-7715

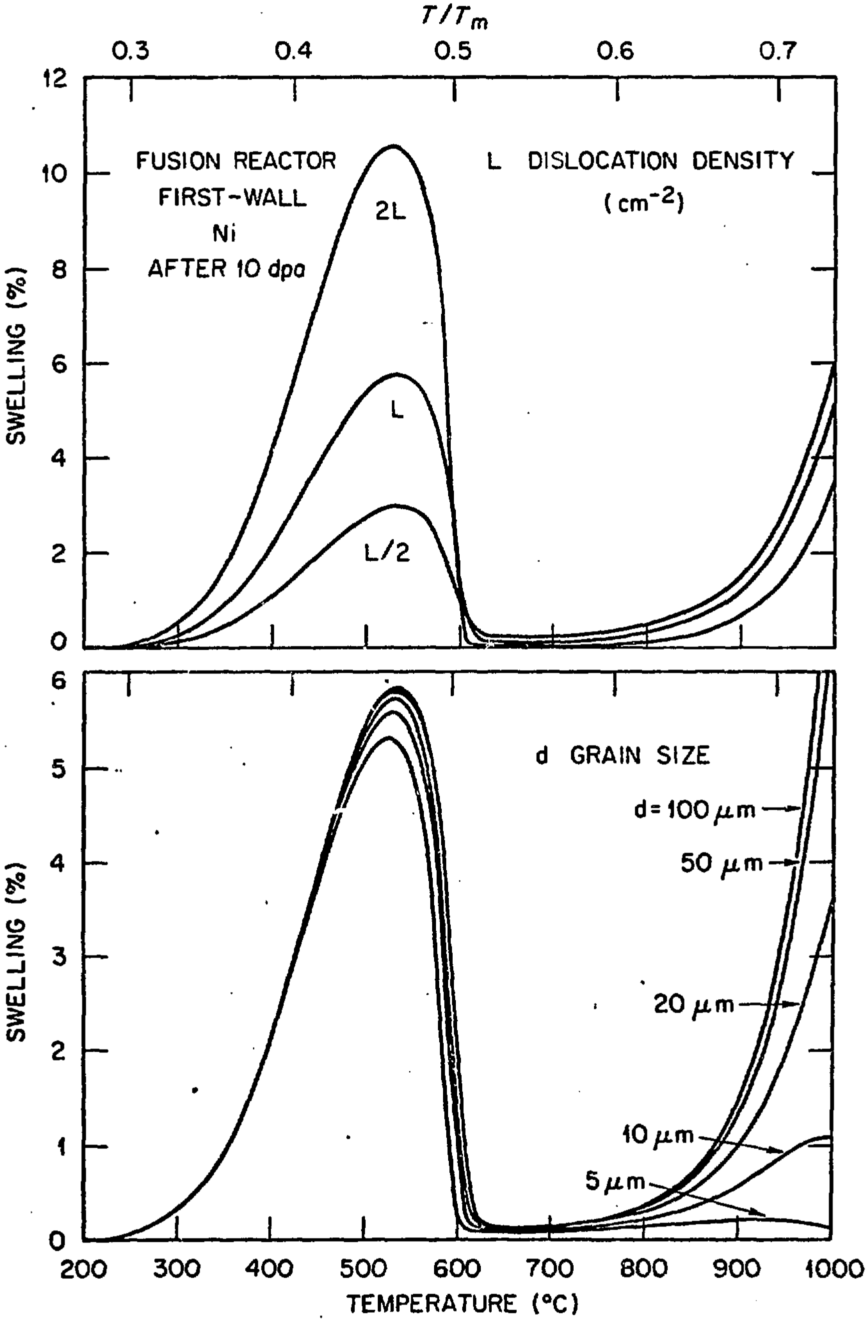

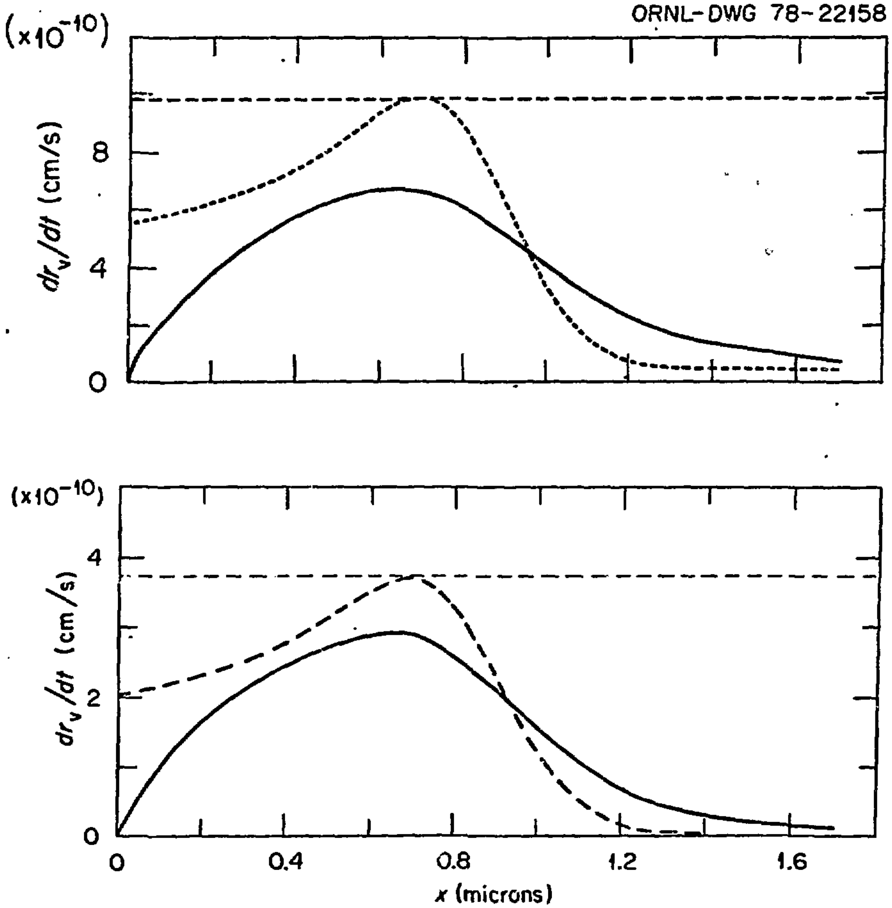
ORNL-DWG 78-22158
(x10^{-10})
8
4
0
dr_v/dt (cm/s)
(x10^{-10})
4
2
0
dr_v/dt (cm/s)
0
0.4
0.8
1.2
1.6
x (microns)

ORNL-DWG 79-7413

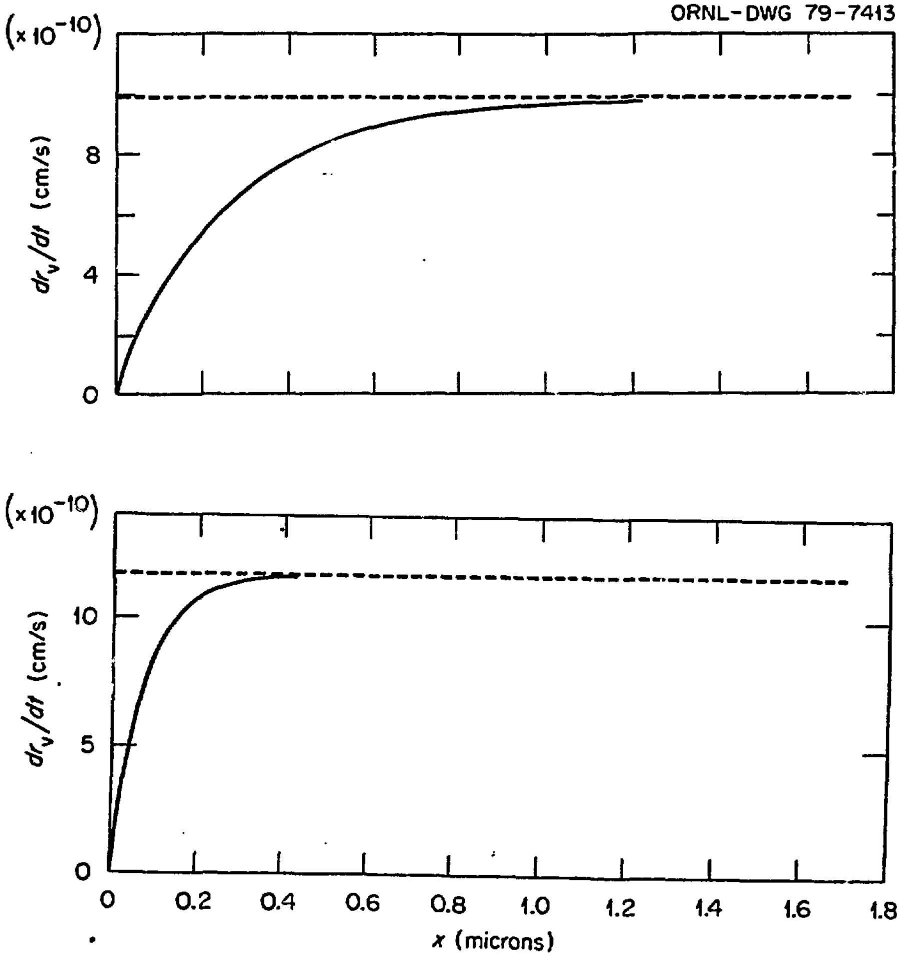

ORNL–DWG 78-21495

MOBILE HELIUM GENERATED DURING NEUTRON IRRADIATION INCREASES SWELLING AT HIGH TEMPERATURES

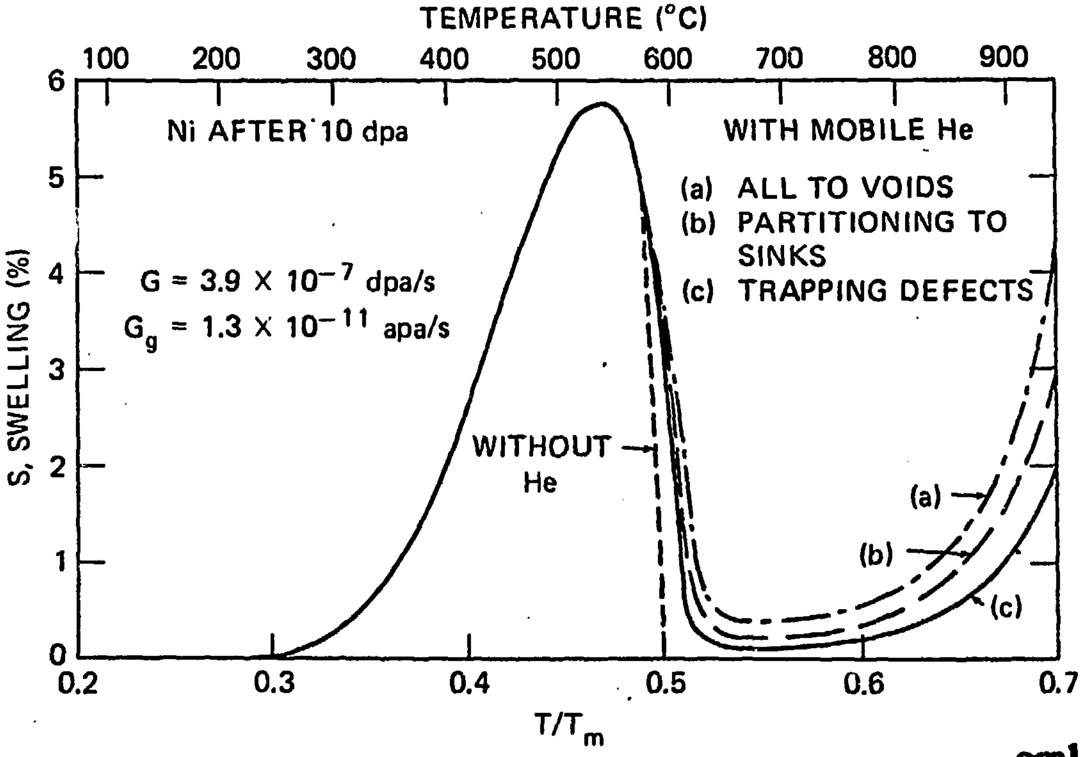

ORNL-DWG 78-21648

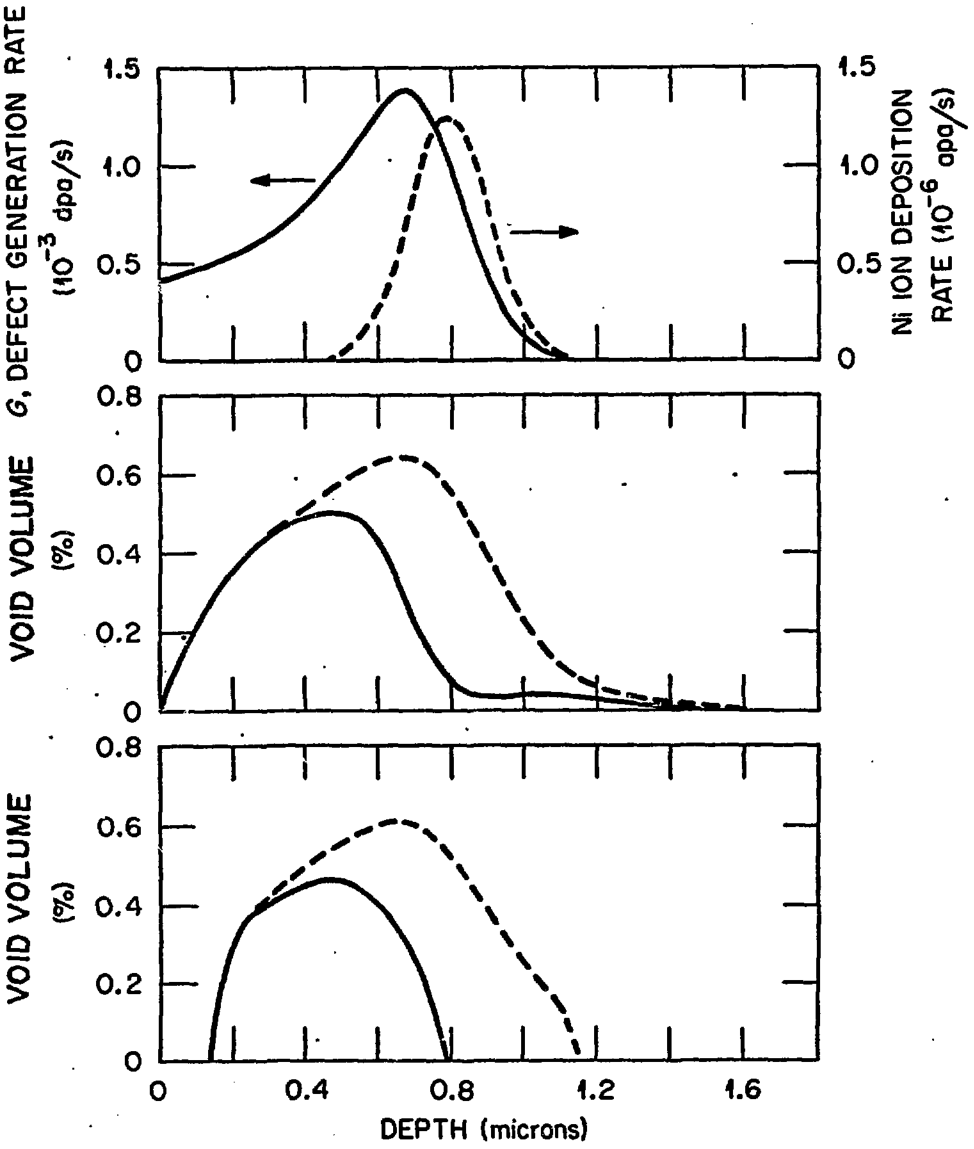

ORNL-DWG 78-22415

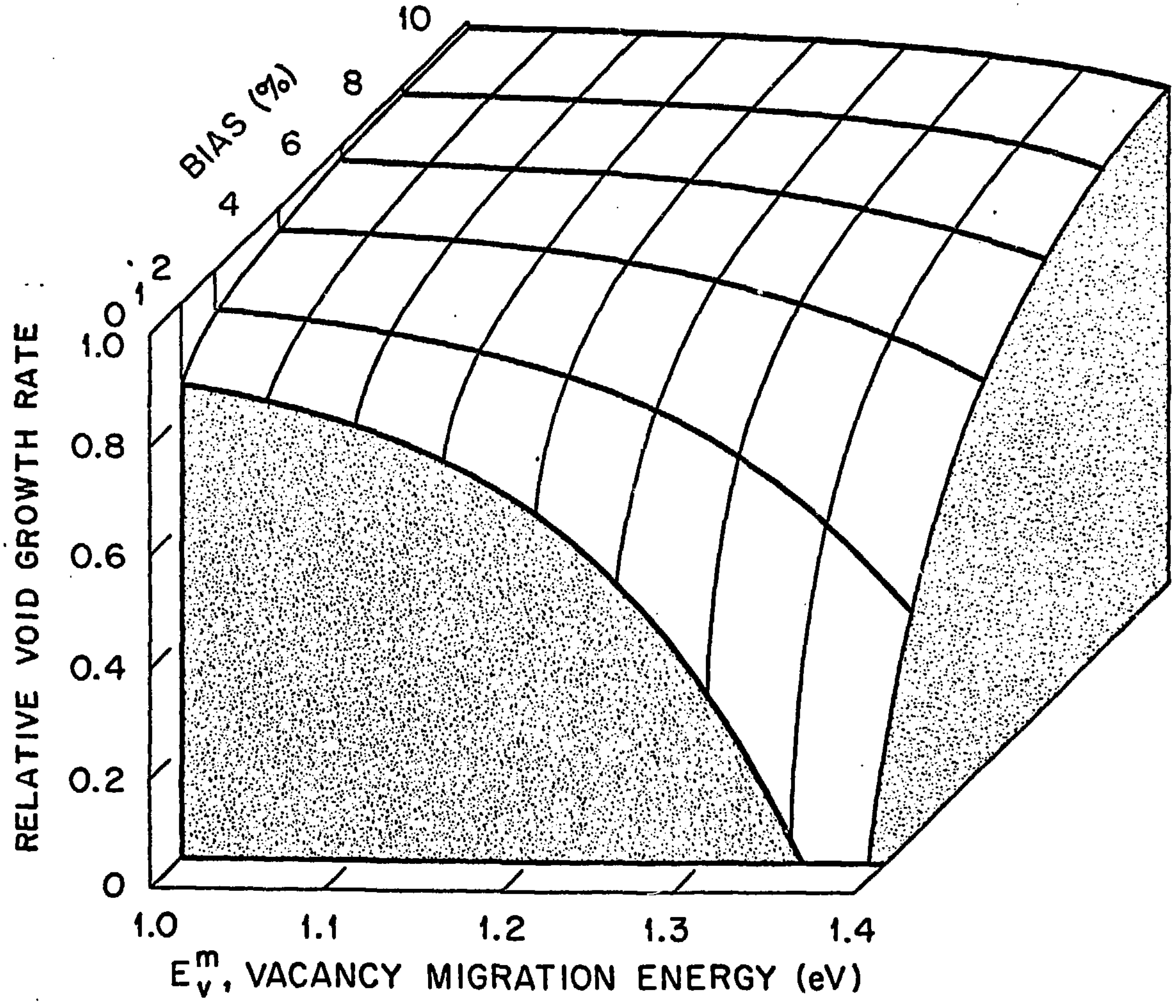

ORNL-DWG 78-22413